Neuron, Volume *90*

Supplemental Information

Cholinergic Mesopontine Signals Govern Locomotion and Reward through Dissociable Midbrain Pathways

Cheng Xiao, Jounhong Ryan Cho, Chunyi Zhou, Jennifer B. Treweek, Ken Chan, Sheri L. McKinney, Bin Yang, and Viviana Gradinaru

Supplementary figures

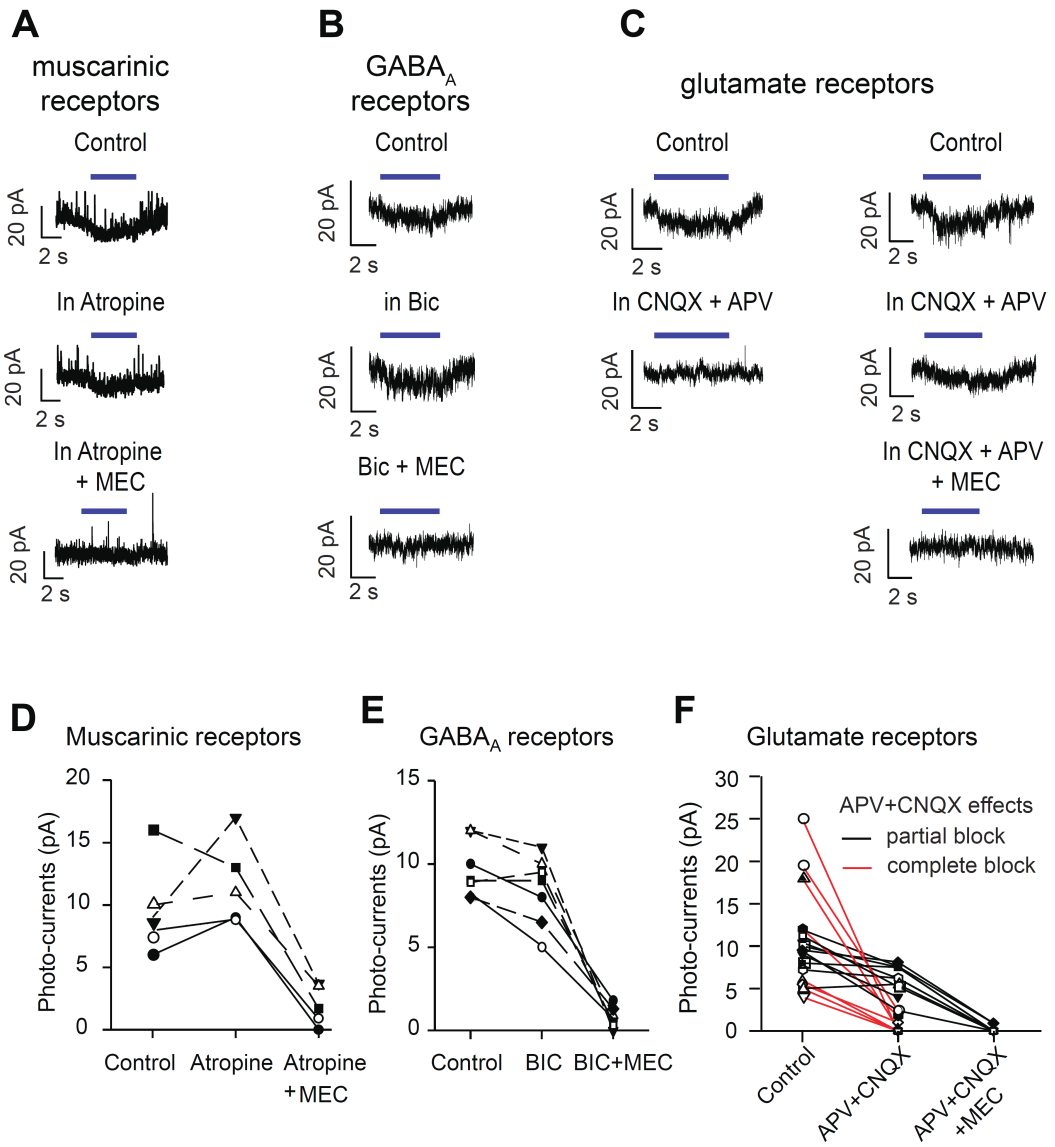

Fig. S1, related to Fig. 1, Characterization of PPN-to-midbrain ChAT transmission. Whole-cell patch-clamp recordings were performed in brain slices from rats with ChR2-eYFP transduced in PPN ChAT neurons. **(A)** A typical inward current in a midbrain neuron (V_H = -50 mV) induced by photo-excitation of ChAT terminals was not blocked by atropine (1 μM), but was abolished by the addition of MEC (10 μM). **(B)** In a typical midbrain neuron, the photoexcitation-induced current was blocked by MEC, instead of bicuculline (10 μM). **(C)** In two typical midbrain neurons, glutamate antagonists (50 μM APV + 20 μM CNQX) abolished inward currents in one neuron, while reduced inward current in another neuron. Addition of MEC abolished the remaining current. **(D-E)** Neither atropine **(D)** nor bicuculline **(E)** reduced inward currents evoked by photo-excitation of PPN-to-midbrain projections, but the currents were blocked by MEC. **(F)** APV + CNQX partially (black lines) or completely (red lines) blocked the inward currents in midbrain neurons, while MEC blocked the remaining currents.

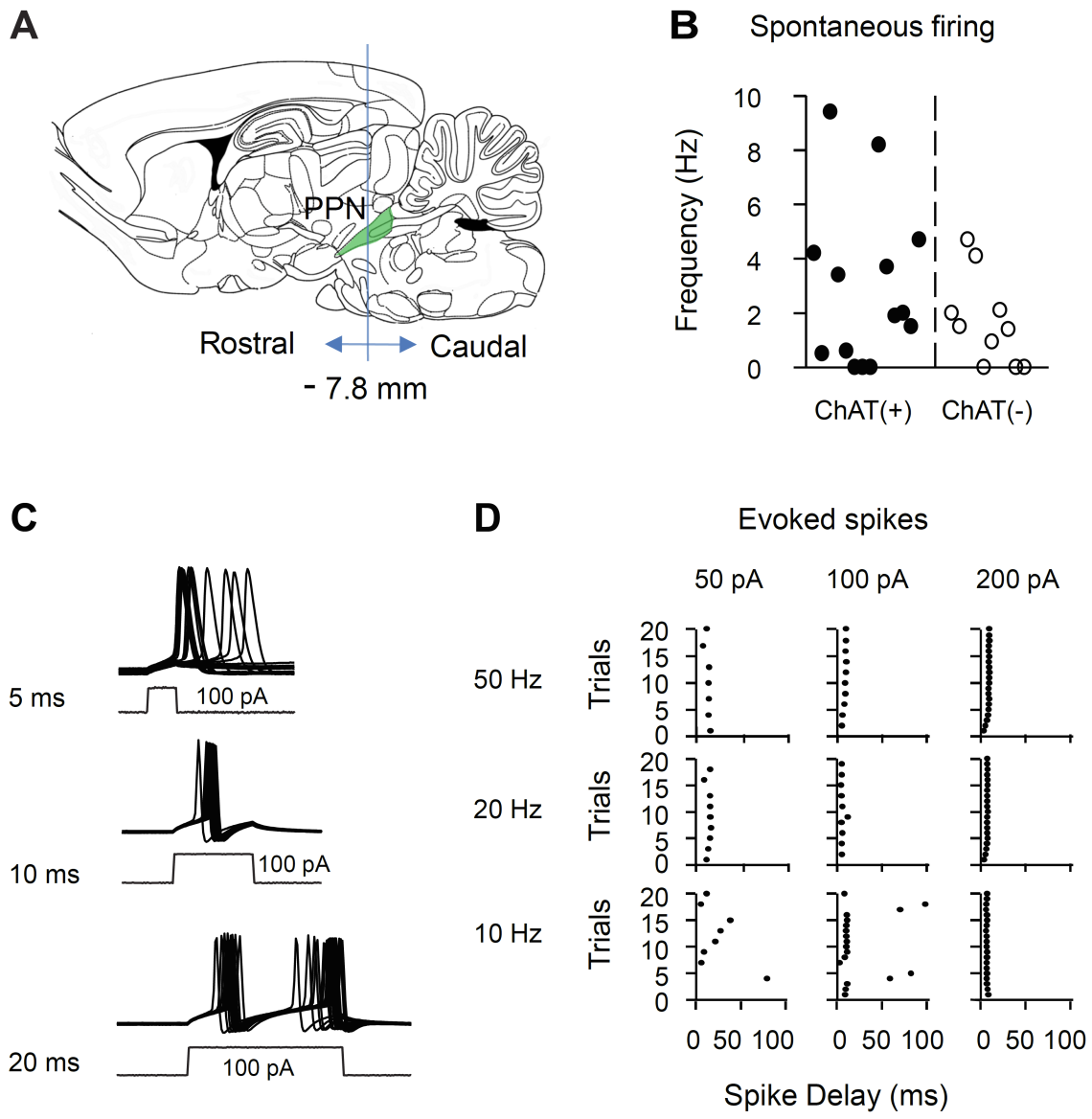

Fig. S2, related to Fig. 2, Electrophysiological properties of ChAT neurons in the PPN. (A) Diagram showing the rostral and caudal PPN. **(B)** Spontaneous firing rates of PPN neurons in brain slices. **(C)** Representative traces from a PPN neuron stimulated by injecting a 100 pA depolarizing current at 10 Hz. The spike delay varied with stimulation durations (top: 5 ms; middle: 10 ms; bottom: 20 ms). **(D)** Typical scatter plots of spike delay in response to 10 ms injection of 50 – 200 pA currents at 10, 20, and 50 Hz.

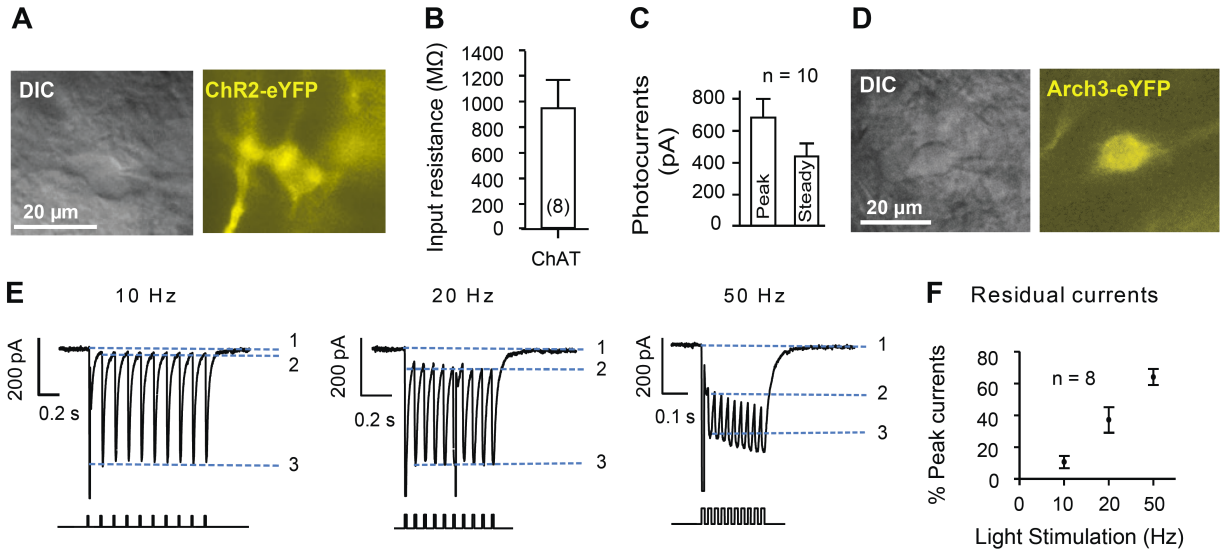

Fig. S3, related to Fig. 3, Optogenetic modulation of PPN ChAT neurons. (A) eYFP expression guided recordings from ChR2-expressing PPN ChAT neurons in brain slices. **(B)** Input resistance of ChAT neurons (952 ± 220 MΩ, n = 8). **(C)** Average light-evoked currents (peak: 682 ± 117 pA; steady state: 439 ± 81 pA; n = 10). **(D)** EYFP expression guided recordings from Arch3-expressing PPN ChAT neurons in brain slices. **(E)** Repetitive light stimuli induced inward currents (V_H = -50 mV) and residual currents between consecutive light stimuli (blue light, 3.1 mW/mm^2, 10 ms). The residual current is the difference between levels 1 and 2 (blue dashed lines). The full current is the difference between levels 1 and 3 (blue dashed lines). **(F)** Summary of the ratio of residual currents to full currents. Summarized data are shown as Mean ± SEM.

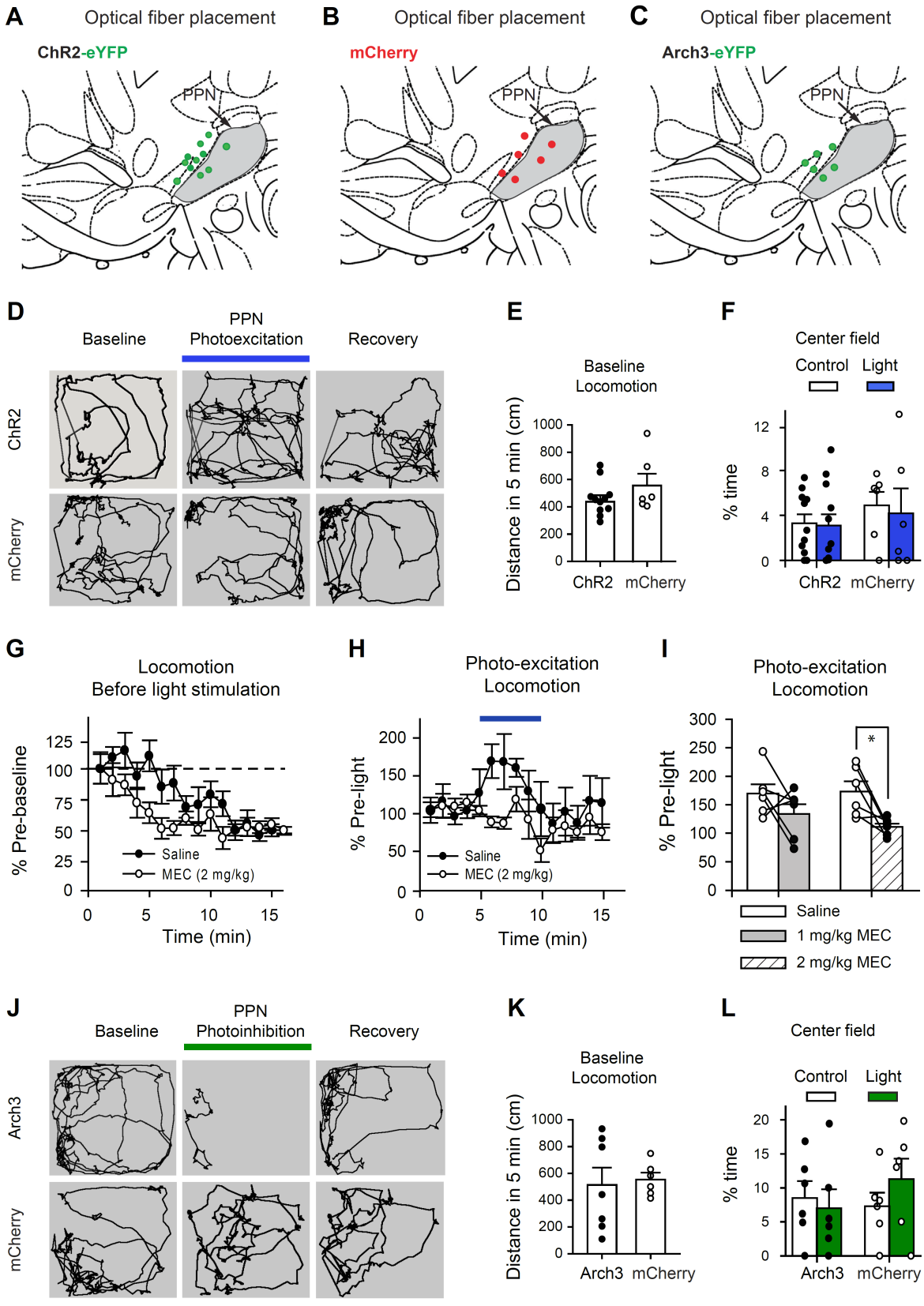
A
Optical fiber placement
ChR2-eYFP
PPN
B
Optical fiber placement
mCherry
PPN
C
Optical fiber placement
Arch3-eYFP
PPN
D
Baseline
PPN
Photoexcitation
Recovery
ChR2
mCherry
E
Baseline
Locomotion
Distance in 5 min (cm)
1000
800
600
400
200
0
ChR2
mCherry
F
Center field
Control
Light
% time
12
8
4
0
ChR2
mCherry
G
Locomotion
Before light stimulation
% Pre-baseline
125
100
75
50
25
0
Saline
MEC (2 mg/kg)
0
5
10
15
Time (min)
H
Photo-excitation
Locomotion
% Pre-light
200
150
100
50
0
Saline
MEC (2 mg/kg)
0
5
10
15
Time (min)
I
Photo-excitation
Locomotion
% Pre-light
300
250
200
150
100
50
0
*
Saline
1 mg/kg MEC
2 mg/kg MEC
J
Baseline
PPN
Photoinhibition
Recovery
Arch3
mCherry
K
Baseline
Locomotion
Distance in 5 min (cm)
1000
800
600
400
200
0
Arch3
mCherry
L
Center field
Control
Light
% time
20
15
10
5
0
Arch3
mCherry

Fig. S4, related to Fig. 4, Control of locomotion by photo-modulation of PPN ChAT neurons. **(A-C)** ChAT-Cre rats were injected with AAV5-DIO-*ChR2-eYFP*, AAV5-DIO-*Arch3-eYFP*, or AAV5-DIO-*mCherry* in the PPN. Optical fiber guides were implanted bilaterally above the PPN. The estimated position of fiber implant tips (green or red dots) in ChR2 **(A)**, mCherry **(B)**, and Arch3 **(C)** rats are shown in a parasagittal anatomical diagram. **(D)** The activity of ChR2 (upper panels) and mCherry (lower panels) rats in an open field arena was tracked before, during, and after blue light stimulation (10 ms, 20 Hz, 5 min). **(E)** Baseline locomotion (5 min) of ChR2 and mCherry rats was at the same levels (ChR2: (437 ± 47) cm, n = 11; mCherry: (571 + 56) cm, n = 10, Shapiro-Wilk Normality Test, $p = 0.437$; *t*-test: $t = 1.83$, $p = 0.1$). **(F)** In both ChR2 and mCherry rats, 5 min blue light stimulation did not change time that the rats traveled through the center area (ChR2: before light (4.2 ± 1.5)%, during light (4.8 ± 1.3)%, n = 11, paired *t*-test, $t = 0.5$, $p = 0.62$; mCherry: before light (4.9 ± 1.2)%, during light (4.2 ± 2.2), n = 6, normality test, $p = 0.34$, paired t-test, $t = 0.35$, $p = 0.74$). **(G-I)** Open field tests were performed in ChR2 rats injected intraperitoneally (i.p.) with vehicle (isotonic sterilized saline) and 1, 2 mg/kg MEC (Matta et al., 2007), and then recorded for open field exploration. Each rat was tested under two treatment conditions, with saline and MEC injections spaced two days apart. Baseline activity was recorded 15 min after saline and MEC injections to allow systemically administered MEC reach the effective concentration in the brain. **(G)** ChR2 rats were placed in open field arena 5 min after 2 mg/kg MEC (open circle) or saline (solid circle) injection, and habituated within 6 and 11 min respectively. **(H)** Injection of 2 mg/kg MEC blocked hyperactivity following photo-excitation of PPN ChAT neurons. Blue light (10 ms) was delivered at 20 Hz for 5 min. **(I)** Summary of photo-excitation's effects on locomotion after saline and MEC injection (Saline vs. 1 mg/kg MEC (saline: (170 ± 16%) of baseline; MEC: (134 ± 17%) of baseline, paired t-test: t = 1.4, p = 0.22); Saline vs. 2 mg/kg MEC (saline: (173 ± 18)% of baseline; MEC: (111 ± 6)%, n = 6, Paired *t*-test, $t = 3.02$, $p = 0.03$)). * $p < 0.05$. **(J)** The activity of Arch3 (upper panels) and mCherry (lower panels) rats was traced before, during, and after green light stimulation (5 min constant). **(K)** Baseline locomotion of ChR2 and mCherry rats was at the same levels; Ach3: (514 ± 129) cm, n = 6; mCherry: (554 ± 51) cm, n = 6; Mann-Whitney U Statistic = 19, T = 44, $p = 0.84$). **(L)** Green light stimulation did not change the time that the rats traveled through the center area (Arch3: before light (8.5 ± 2.5)%, during light (7 ± 2.8)%, n = 6, paired *t*-test, $t = 0.7$, $p = 0.52$; mCherry: before light (7.3 ± 2.8)%, during light (11.3 ± 3), n = 6, paired *t*-test, $t = 2.1$, $p = 0.09$). Summarized data are shown as Mean ± SEM.

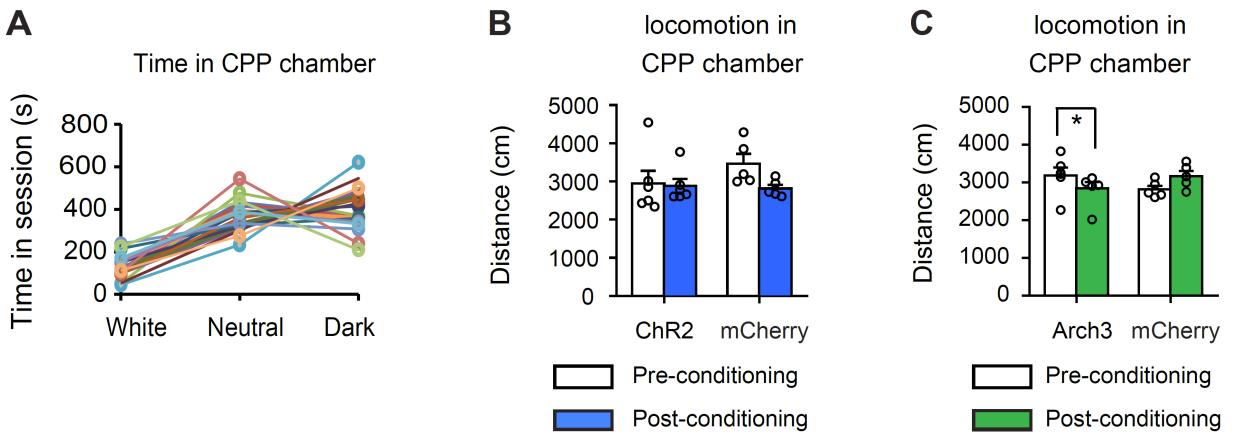

Fig. S5, related to Fig. 4, Locomotion during pre- and post-conditioning sessions in conditioned place preference. (A) The total time rats spent in each compartment during the 15 min preconditioning exploration period (white: (109 ± 14) s; dark: (433 ± 24) s; paired *t*-test: t = 9.42, $p < 0.0001$). **(B)** Blue light conditioning did not change movement distance in the CPP chamber during 15 min pre- and post-conditioning sessions. ChR2: Pre-conditioning, (2938 ± 337) cm; Post-conditioning, (2811 ± 98) cm, n = 6, t = 0.29, p = 0.78, paired *t*-test. mCherry: Pre-conditioning, (3462 ± 256) cm; Post-conditioning: (2880 ± 183) cm, n = 5, t = 2.34. p = 0.08, paired t-test. **(C)** Green light conditioning reduced movement in Arch3 injected rats, but not in mCherry injected rats. Arch3: Pre-conditioning: (3182 ± 210) cm; Post-conditioning: (2840 ± 170) cm, n = 6, t = 3.7, p = 0.014. mCherry: Pre-conditioning: (2811 ± 98) cm, Post-conditioning: (3164 ± 142) cm, n = 5, t = 2.05, p = 0.11. Summarized data are shown as Mean ± SEM.

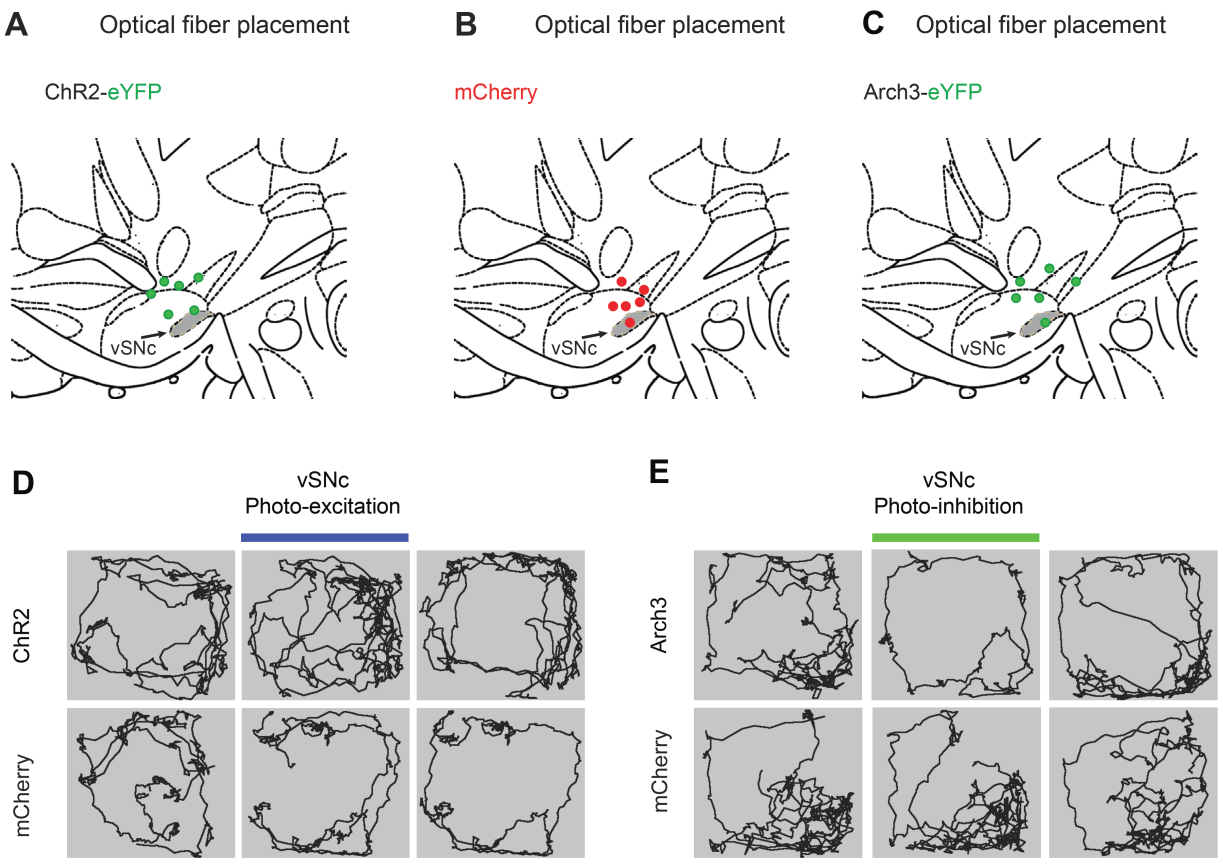

Fig. S6, related to Fig. 5, Optogenetic modulation of PPN-to-vSNc projections and locomotion. (A-C) ChAT-Cre rats were injected with AAV5-DIO-*ChR2-eYFP*, AAV5-DIO-*Arch3-eYFP*, or AAV5-DIO-*eYFP* in the PPN. Optical fiber guides were implanted bilaterally above the vSNc to modulate PPN-to-vSNc ChAT connections. The estimated position of fiber implant tips in (green dots) ChR2 **(A)**, mCherry **(B)**, and Arch3 **(C)** rats are shown in a parasagittal anatomical diagram. **(D)** Typical movement tracks of a ChR2 rat (upper panels) and a mCherry rat (lower panels) before, during and after photo-stimulation of PPN-to-vSNc connections (blue light: 10 ms, 20 Hz, 5 min, 9 xiao april 4 /mm^2). **(E)** Typical movement tracks of an Arch3 rat (upper panels) and a mCherry rat (lower panels) before, during and after photo-inhibition of PPN-to-vSNc connections (green light: 5 min, 5 mW/mm^2). Summarized data are shown as Mean ± SEM.

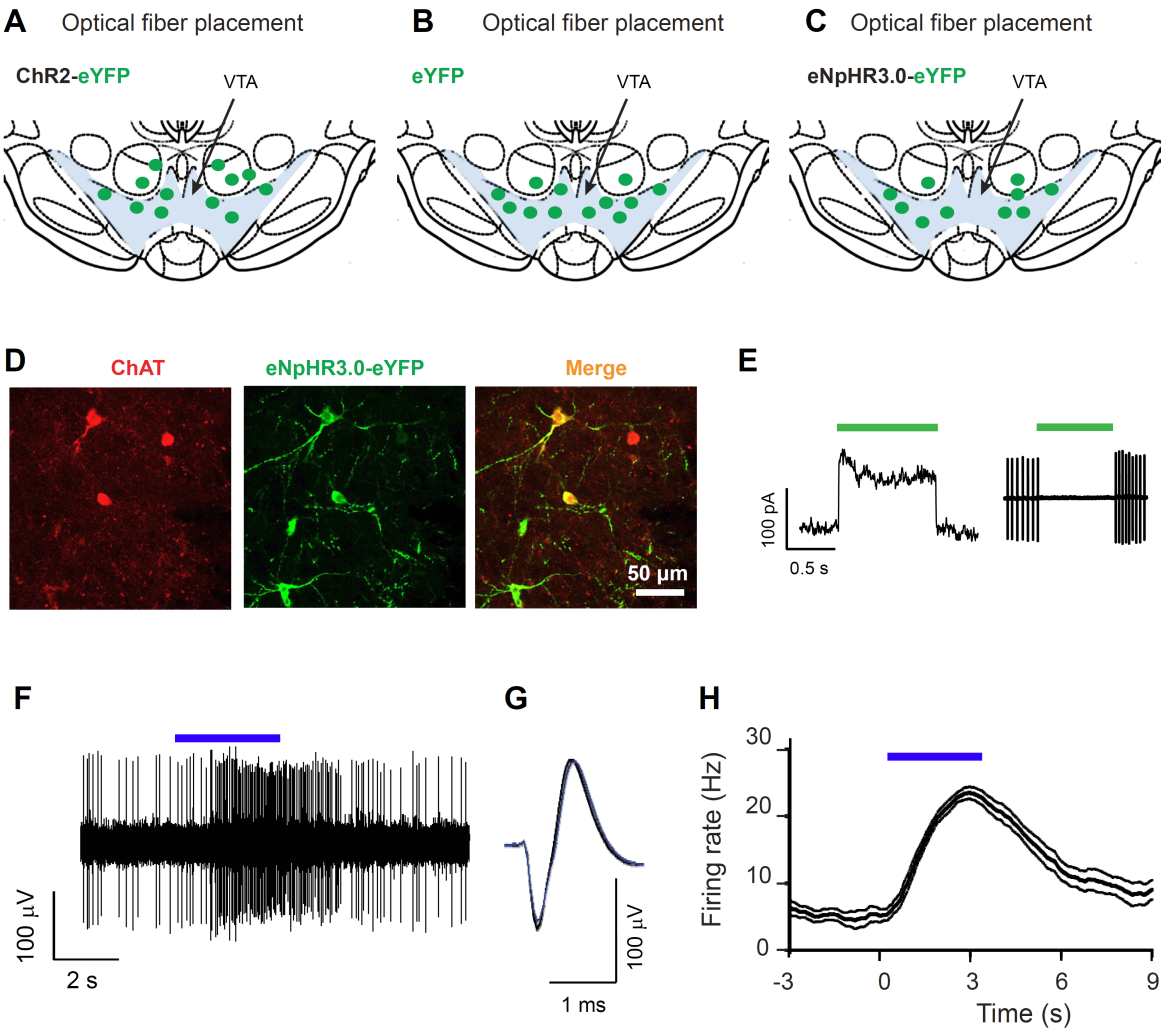

Fig. S7, related to Fig. 6, Optogenetic modulation of PPN-to-VTA ChAT connections. (A-C) ChAT-Cre rats were injected with AAV5-DIO-*ChR2-eYFP*, AAV5-DIO-*eYFP*, or AAV5-DIO-*eNpHR3.0-eYFP* in the PPN. Optical fiber guides were implanted bilaterally above or in the VTA to modulate PPN-to-VTA ChAT connections. The estimated position of fiber implant tips (green dots) in ChR2 **(A)**, eYFP **(B)**, and eNpHR3.0 **(C)** rats were shown in a parasagittal anatomical diagram. **(D)** AAV5-DIO-*eNpHR3.0-eYFP* was delivered to the PPN of ChAT-Cre rats. The eNpHR3.0-eYFP-positive neurons were ChAT-positive. The *eNpHR3.0-eYFP* was transduced into ~60% of ChAT neurons. **(E)** Green light (9 mW/mm^2) induced an outward current (left, V_H = -50 mV), and silenced activity (right, cell-attached mode) in a representative eNpHR3.0-containing neuron. **(F-H)** Optrode recordings from the VTA (ML: −0.6 mm, AP: −5.8 mm, DV: 8.2 mm) were performed in an anesthetized ChAT-Cre rat, injected with AAV5-DIO-*ChR2-eYFP* in the PPN and recovered for two months. **(F)** Photo-excitation (20 Hz, 10 ms, for 3 seconds; 4.73 mW/mm^2, 0.5 mm below the tip of the optical fiber) increased the frequency of single-unit activity in the VTA. **(G)** Photo-excitation did not change spike waveforms (Black: before photo-excitation; Blue: during photo-excitation). **(H)** Average firing rates before, during, and after photo-excitation (pooled from 8 trials). Data are represented as mean ± SEM.

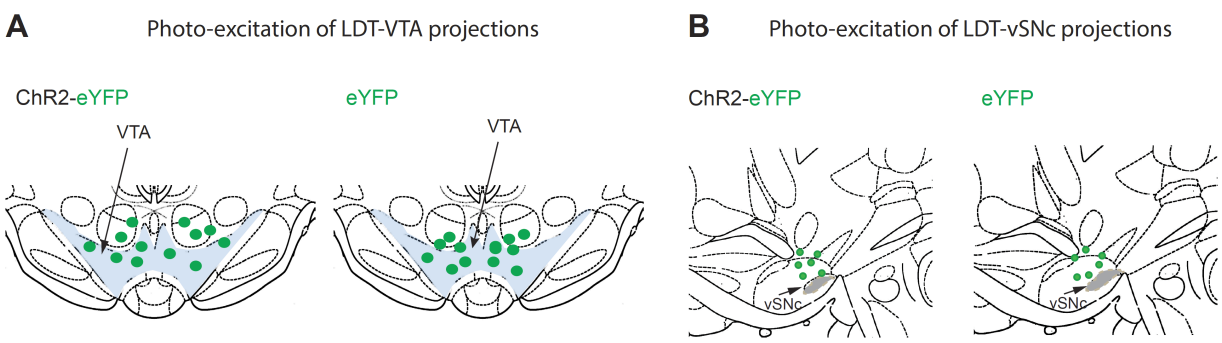

Currents in midbrain neurons induced by LDT ChAT photo-excitation

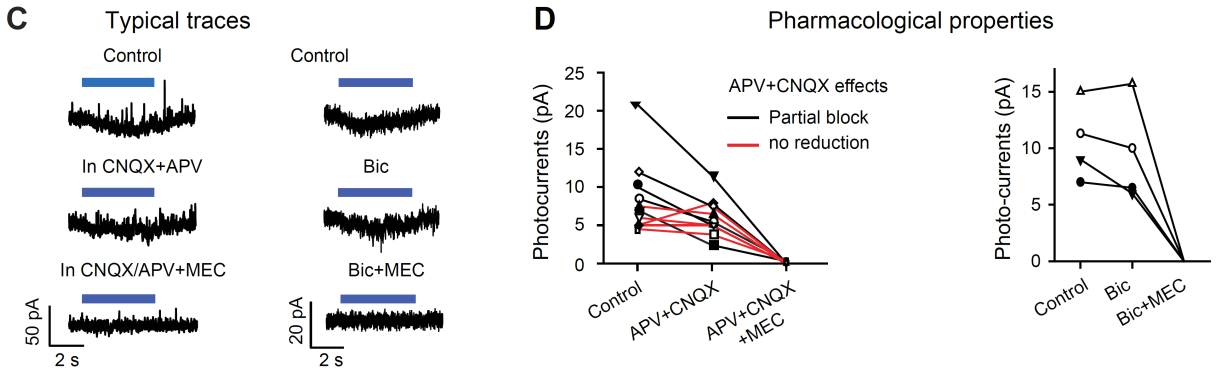

Neuronal tracing of PPN and LDT ChAT projections

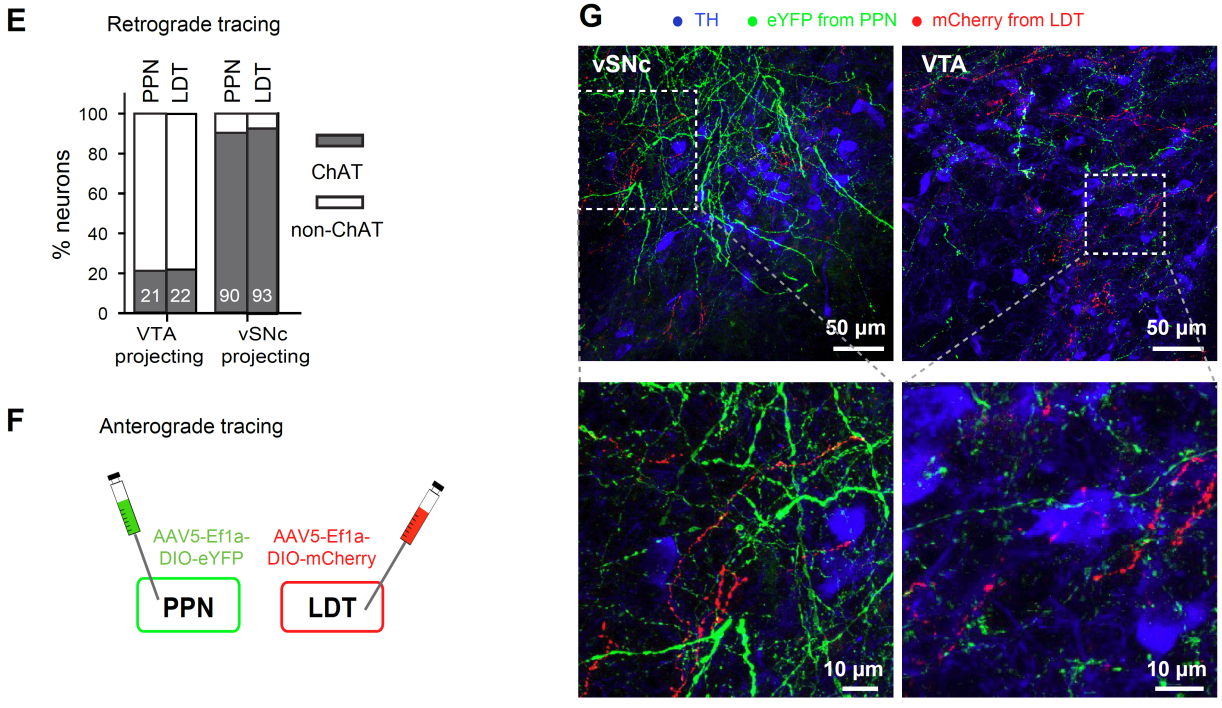

Fig. S8, related to Fig. 7 and 8, LDT-to-midbrain ChAT connection. (A-B) For photo-excitation of LDT-to-VTA and LDT-to-vSNc, we delivered AAV5-DIO-*ChR2-eYFP* and AAV5-DIO-*eYFP* into the LDT of ChAT-Cre rats, and implanted optical fiber guides bilaterally in / above the VTA and the vSNc. The positions of optical fiber tips in the VTA and the vSNc are respectively shown in **(A)** and **(B)**. **(C)** Typical photocurrents in two midbrain neurons (V_H = -50 mV) induced by photo-excitation of LDT-to-vSNc/VTA ChAT terminals. The photocurrents were partially blocked by 50 μM APV + 20 μM CNQX, but not 10 μM Bic. 10 μM MEC blocked the currents. **(D)** Summary of photocurrent amplitude before, during application of APV+CNQX, APV+CNQX+MEC, BIC, and BIC+MEC. **(E)** In the PPN and LDT, a minority of VTA projecting neurons were cholinergic; in contrast, a great majority of vSNc projecting neurons were cholinergic. **(F)** For anterograde tracing, AAV5-DIO-*eYFP* and AAV5-DIO-*mCherry* were respectively delivered to the PPN and LDT of the same ChAT-Cre rats to trace ChAT projections to the VTA and vSNc. **(G)** ChAT fibers from both the LDT (red) and the PPN (green) intermingled adjacent to dopaminergic neurons (blue) in the vSNc (left panels) and the VTA (right panels). The insets (lower panels) show that both vSNc and VTA dopaminergic neurons had cholinergic fibers from the PPN and LDT in their proximity.

Supplementary Tables

Table S1, related to Fig. 2, Electrophysiological properties of PPN neurons.

Parameters	ChAT (+) (*n* = 14)	ChAT (-) (*n* = 8)	*t* value	*p* value
Spontaneous Firing Rate (Hz)	2.8 ± 1.2	2.1 ± 0.6	1.78	0.49
Firing Jitter	0.40 ± 0.09	0.52 ± 0.15	0.51	0.61
AP Width (ms)	1.4 ± 0.2	1.5 ± 0.2	0.33	0.74
Saturating Firing Rate (Hz)	56 ± 11	32 ± 3.3	3.35	0.015 *
AHP (mV)	-17.6 ± 1.5	-16.8 ±1.5	0.73	0.48
Vm (mV)	-50 ± 1.6	-54 ± 3.4	1.30	0.23
Rm (MΩ)	766 ± 113	308 ± 52	3.31	0.006 **

AP: action potential; AHP: afterhyperpolarization; Vm: membrane potential; Rm: membrane resistance. Data are shown as mean ± SEM.

Table S2, related to Fig. 2, Variations of spike delay in PPN ChAT and non-ChAT neurons.

Neurons	Currents (pA)	10 Hz	20 Hz	50 Hz	Statistics	P value
ChAT	50	0.57+0.16	0.28+0.04	0.3+0.06	F = 5.2	0.01
n = 9	100	0.27+0.13	0.27+0.13	0.2+0.02	F = 0.14	0.87
	150	0.12+0.02	0.14+0.01	0.21+0.03	F = 3.79	0.04
	200		0.15+0.02	0.16+0.03	t = 0.35	0.37
Non-ChAT	50	0.80+0.17	0.18+0.03	0.24+0.08	F = 9.49	0.004
n = 5	100	0.21+0.06	0.22+0.02	0.23+0.02	F= 0.09	0.92
	150	0.18+0.07	0.14+0.02	0.23+0.03	F = 1.11	0.36
	200	0.10+0.01	0.16+0.03	0.23+0.03	F = 5.59	0.02
	250		0.12+0.02	0.16+0.02	t = 1.42	0.10

Variations of spike delay were calculated with standard deviations divided by their means. Data are shown as mean ± SEM.

Supplementary Experimental Procedures

Animals

We used Long Evans wild type and Choline acetyl-transferase (ChAT)-Cre rats (Witten et al., 2011). We used ChAT-Cre rats rather than mice, because of the rat's larger brain size and well-defined SNc tiers (Paxinos and Watson, 2006, 2012), which enable better optical isolation of each tier. Animal husbandry and all experimental procedures involving rats were approved by the Institutional Animal Care and Use Committee (IACUC) and by the Office of Laboratory Animal Resources at the California Institute of Technology under IACUC protocol 1650. After weaning age, rats were double-housed with *ad libitum* access to food and water until surgery (3 month old). Following surgery, rats were single-housed on a 12 hours light/dark cycle (light on: 6 PM) until behavioral testing (4-6 months old) or until electrophysiological recordings (4-5 months old).

Surgeries for viral delivery and optical fiber implantation

The rats were anesthetized with 2% isofluorane gas/carbogen mixture and stabilized on a stereotaxic frame (Kopf Instruments). A midline incision was made down the scalp, and 0.5 mm diameter holes were bilaterally drilled above the pedunculopontine nucleus (PPN) (anteroposterior (AP): -8.0 mm; mediolateral (ML): ±2.0 mm) and the laterodorsal tegmental nucleus (LDT) (AP): -8.8 mm; mediolateral (ML): ±0.8 mm). All stereotaxic coordinates are described relative to bregma. Adeno-associated viral vector serotype 5 (AAV5) carrying Ef1α promoter-driven Cre-dependent (*Ef1α*-DIO) *ChR2-eYFP* or *Ef1α*-DIO-*Arch3.0-eYFP* or *Ef1α*-DIO-*mCherry* or *Ef1α*-DIO-*eYFP* or *Ef1α*-DIO-*eNpHR3.0-eYFP* (0.8 µL, viral concentration is 2-4x10^{12} genome copies, UNC Vector Core) was injected at dorsoventral (DV) 7.2 mm for the PPN and 7.0 mm for the LDT. After infusion, rats were either allowed 4 weeks recovery in advance of brain slice patch-clamp recordings, or rats were prepared for *in vivo* optogenetic modulation as described below. The available heterozygous male ChAT-cre rats were alternatively assigned to one of the testing groups to assure that the rats in groups have similar ages for behavioral tests.

For *in vivo* optogenetic modulation of PPN ChAT neurons, immediately after virus injection, we bilaterally implanted custom-made optical fiber (300 µm in diameter, NA 0.39, Thorlabs) implants (light-transmission: 55-70%) with tips 0.3 mm above the virus injection site. To deliver light to ChAT terminals in the ventral substantia nigra pars compacta (vSNc), optical fibers were inserted bilaterally above the vSNc (AP: -6.4 mm; ML: ±2 mm; DV: 7.7 mm) (Fig. 5B). To deliver light to ChAT terminals in the ventral tegmental area (VTA), optical fibers were inserted bilaterally above the VTA with a ±10 degree angle relative to dorsal-ventral axis from the holes in the skull (AP: -6.2 mm; ML: ±2 mm) to reach (AP: -6.2 mm; ML: ±0.6-0.8 mm; DV: 7.8 mm) (Fig. 6B). Fibers were adhered to the skull with dental cement (C&B Metabond, Parkell), the incision was sutured closed, and animals were monitored closely during recovery. Behavioral experiments commenced 1-2 months following subject surgical preparation to allow for complete viral transduction of PPN neurons and their midbrain projections. Behavioral control cohorts were comprised of rats injected with viral vectors for the *mCherry* or *eYFP* alone.

Surgeries for retrograde neuronal tracing

Long Evans wild type and ChAT-Cre rats (3-5 months old, female or male) were prepared for delivery of retrogradely traveling virus as described in the surgery section above. Briefly, the rats were anesthetized with 2% isofluorane gas/carbogen mixture and stabilized on a stereotaxic frame (Kopf Instruments). 0.5 mm diameter holes were bilaterally drilled above the left VTA (AP: -5.8 mm; ML: -0.6 mm) and vSNc (AP: -6.1 mm; ML: -2.1 mm). Herpes simplex viruses that carry *eYFP-Cre* and *mCherry-Cre* transgenes under humanized *Ef1a* promoter (HSV-*hEf1a-eYFP-Cre* and HSV-*hEF1a-mCherry-Cre*, 1.5 µL, viral concentration is $3x10^8$ genome copies/mL, MIT Viral Gene Transfer Core) were stereotaxically delivered into the VTA (DV: -8.2 mm) and vSNc (DV: -8.1 mm), respectively. Virus was slowly injected at 100 nL/min rate for 15 minutes and additional 10 min was allowed for diffusion and to avoid backflow of virus along the track. Rats were housed for a total of 3 weeks from the surgery date to allow maximal viral expression, and then were sacrificed. Their brains were fixed in 4% paraformaldehyde for 4-5 hours at 4 °C and sectioned into 50 µm coronal sections. From each rat we collected 4 sections (50 µm) containing the PPN (2 from anterior (AP: -7.6 mm) and other 2 from posterior (AP: -8.4 mm), see Fig. S2), and also collected 2 sections (AP: -8.5 mm and -9 mm) containing the LDT. PPN and LDT ChAT neurons were visualized with ChAT-antibody staining. We imaged neurons containing eYFP, mCherry, and ChAT in the PPN and LDT regions of the left hemisphere (HSV injection side) under a confocal microscope equipped with a 25x water immersion objective. We manually counted the cells containing eYFP, mCherry, ChAT or their combinations.

Electrophysiological recordings

Brain slice preparation

Electrophysiological recordings were performed on parasagittal brain slices, using the protocol described (Xiao et al., 2015; Ye et al., 2006) with some modifications. Previous electrophysiological studies using Sprague Dawley rats (3-10 wks old) revealed heterogeneity in membrane conductance and ion channels for ChAT and non-ChAT neurons in the PPN (Kang and Kitai, 1990; Takakusaki et al., 1997; Takakusaki et al., 1996). We used 2-3 months old naive wild-type (WT) Long Evans rats to characterize membrane properties of ChAT and non-ChAT neurons, and used 4-6 months old ChAT-Cre rats (Long-Evans background) injected with viral vectors in the PPN to define the responses of PPN ChAT neurons and midbrain neurons to optogenetic modulation. In brief, the rats were euthanized with carbon dioxide, and were subjected to cardiac perfusion with ice-cold modified glycerol-based artificial cerebral spinal fluid (gACSF) saturated with 95% O_2 / 5% CO_2 (carbogen) containing (mM): 250 glycerol, 2.5 KCl, 1.2 NaH_2PO_4, 1.2 $MgCl_2$, 2.4 $CaCl_2$, 26 $NaHCO_3$ and 11 glucose. The brain was subsequently removed and sliced with a vibratome (VT-1200, Leica Inc.), while immersed in gACSF. Parasagittal brain slices (350 µm) containing the PPN, the substantia nigra, or the VTA were allowed to recover at 32 °C in a holding chamber filled with carbogenated ACSF, containing (mM): 125 NaCl, 2.5 KCl, 1.2 NaH_2PO_4, 1.2 $MgCl_2$, 2.4 $CaCl_2$, 26 $NaHCO_3$, and 11 glucose. One hour later, the holding chamber with slices was placed at room temperature and the slices were ready for patch-clamp recordings.

Patch-clamp recordings

Slices were transferred to the recording chamber, and perfused (1.5 - 2.0 ml/min) with carbogen-saturated ACSF at 32 ± 0.5 °C. We recorded PPN, substantia nigra and VTA neurons in brain slices. The neurons were visualized with an upright microscope (BX50WI; Olympus) with near infrared or fluorescent (yellow) illumination. Whole-cell patch-clamp techniques were used to record electrophysiological signals with MultiClamp 700B amplifiers (Molecular Devices), Digidata 1440 analog-to-digital converters (Molecular Devices), and pClamp 10.4 software (Molecular Devices). Data were sampled at 10 kHz and filtered at 2 kHz. Patch electrodes had resistance of 4 - 6 MΩ, when filled with intrapipette solution (mM): 135 K gluconate, 5 KCl, 5 EGTA, 0.5 $CaCl_2$, 10 HEPES, 2 Mg-ATP, and 0.1 GTP. The pH of the solution was adjusted to 7.2 with Tris-base, and the osmolarity was adjusted to 300 mOsm with sucrose. The junction potential between patch pipette and bath solution was nulled just before gigaseal formation. Series resistance was monitored without compensation throughout the experiment using the Multiclamp 700B. The data were discarded if the series resistance (15 - 30 MΩ) changed by more than 20% during whole-cell recordings. We recorded 1-2 neurons from each slices and used 3-4 slices from each rat.

In some recordings, we included 0.2% neurobiotin in the intrapipette solution so that the recorded neurons were labeled during whole-cell recordings. The labeled neurons were visualized with Alexa555-conjugated streptavidin, and identified as ChAT and non-ChAT via immunostaining for ChAT (Goat anti-ChAT IgG, Millipore).

Electrophysiological data were analyzed with Clampfit 10.4, Molecular Devices. We used the “event detection” feature to analyze action potentials (spike delay, half-width, afterhyperpolarization, frequency). We applied 5 mV hyperpolarization steps (500 ms) from -50 mV, and calculated membrane input resistance according to Ohm’s law. For light-evoked currents in ChR2-expressing neurons, we measured the peak and steady state current amplitudes within 10 ms and at 500 ms after the initiation of stimulation, respectively. For light-evoked inward currents in SNc and VTA neurons, we measure the peak amplitudes after the traces were low-pass filtered at 500 Hz.

To photo-activate ChR2 and Arch3 in PPN ChAT neurons in brain slices, we used blue (420-455 nm, 3.1 mW/mm^2) and green (520-570 nm, 9 mW/mm^2) light from an LED light source (Lumencor) controlled by Clampex 10.4 (Molecular Devices) through Digidata 1440 (Molecular Devices). The light power (mW) was measured with a power meter (PM100D, ThorLab), and it was converted to light intensity (mW/mm^2). To photo-activate midbrain ChAT terminals from the PPN, we applied 1-10 s blue light. The light-evoked inward currents (>5 pA) and increase of firing rate (>10%) in midbrain neurons indicate the positive ChAT connections.

Optrode recordings

2-3 months following the injection of AAV5-DIO-*ChR2-eYFP* into the PPN, ChAT-Cre rats were anesthetized with isofluorane and stabilized on a stereotaxic frame (Kopf). A midline incision was made down the scalp, and 2 mm diameter holes were bilaterally drilled above the vSNc (AP: 6.1 mm; ML: 2.0 mm). An optrode was made by attaching a 1 MΩ tungsten electrode (AM system) to a 200 μm optical fiber (Thorlab) (Gradinaru et al., 2007). The electrical signals were recorded

from the electrode with an A-M 1800 amplifier (x1000), band-width filtered at 10 Hz (high-pass) – 5 kHz (low-pass), digitized by a data acquisition board (DataWave), and sampled at 20 kHz and saved and processed with SciWorks software 8.02 (Datawave). The optical fiber was connected to a 473 nm laser, TLL-controlled by SciWorks software through the data acquisition board to deliver light pulses (10 ms at 20 Hz; 4.73 mW/mm^2; 0.5 mm below optical fiber tip). We searched for VTA neurons by slowly lowering the optrode to the target coordinates (AP: 5.8 mm; ML: 0.5-1 mm; DV: 7.8 to 8.5 mm). The single-units from the positions within the VTA were included in data analysis.

After recordings, the rats were transcardially perfused with 4% paraformaldehyde (PFA), and the brains were post-fixed in 4% PFA for 3-5 hrs at 4 °C. The brain was sectioned into 100 µm slices and examined to mark the deepest position of optrode insertion; this observation was used to calibrate all other recording sites.

Immunohistochemistry

The rats were euthanized with CO_2 and transcardially perfused with 30 ml PBS with heparin (10 U/ml), and then with 60 ml 4% PFA in PBS. The rat brain was removed from skull, post-fixed in 4% PFA for 3-4 hrs, and then sectioned into 100 µm slices with a vibratome (Leica Inc.). The slices were mounted onto microscope slides (Fisher Scientific), dried at room temperature, and frozen at -20 °C.

For immunohistochemistry, green fluorescent protein (GFP) antibodies (rabbit anti-GFP IgG, Life technologies, Catalogue number: A-11122; chicken anti-GFP IgG, Aves Lab, Catalogue number: GFP-1020) were used to detect the expression of ChR2-eYFP / Arch3.0-eYFP / HSV-hEf1a-eYFP / eNpHR3.0-eYFP; an antibody against ChAT (Goat anti-ChAT IgG, Millipore, Catalogue number: AB144P) was used to identify ChAT neurons; tyrosine hydroxylase (TH) antibodies (mouse anti-TH IgG from Santa Cruz, Catalogue number: sc-25269 or Chicken anti-TH IgG from Aves Lab, Catalogue number: THY) were used to stain DA neurons and mark midbrain nuclei; an mCherry antibody (rabbit anti-mCherry IgG, Abcam, Catalogue number: ab167453) was used to detect the expression of HSV-hEf1a-mCherry. Neurons were also labeled with Nissl stain (NeuroTrace® 435/455 Blue Fluorescent Nissl Stain, Life technologies, Catalogue number: N-21479) (Quinn et al., 1995).

The brain sections were thawed and washed twice (10 min each) with cold PBS (4 °C), permeabilized for 1 hr in PBS / 0.1% Triton-X 100, blocked for 1 hr in PBS / 10% donkey serum, incubated in primary antibodies (1:500 anti-GFP IgG) / (1:200, goat anti-ChAT) / (1:1000, chicken anti-TH antibody) or Alexa555-conjugated streptavidin (1:500, Life Technology) in PBS / 4% donkey serum at 4 °C for 18 hrs, washed 3 times (15 min each) in PBS, incubated in Alexa 488, 561, or 647 conjugated secondary antibodies (1:500, Life Technologies and Jackson ImmunoResearch Lab) in PBS / 4% donkey serum at room temperature for 1 hr. Samples were washed 3 times (10 min each) in PBS, dried at room temperature, and coverslipped with mounting medium (Vector laboratories Inc.).

PACT (Passive CLARITY)

Rat brains were processed with PACT, a tissue clearing and staining protocol (Treweek et al., 2015; Yang et al., 2014). ChAT-Cre rats injected with AAV5-*Ef1α*-DIO-*ChR2-eYFP* in the PPN were euthanized, and the brains were fixed as described in "Immunohistochemistry" above. After complete rinse of PFA with 0.01 M PBS, the brain was placed in a brain matrix (ASI Instruments) with 1 mm grids, and was cut into 1 or 2 mm thick parasagittal or coronal sections with razor blades. The brain sections were placed in PBS, 4% acrylamide, 0.25% VA-04 thermal initiator, and were incubated overnight at 4 °C. To polymerize acrylamide, nitrogen gas was bubbled into the acrylamide solution for 1 min to remove oxygen and then the samples were incubated in a 37 °C water bath for 1-2 hrs until the solution became viscous. Then, the brain sections were rinsed with PBS 3 times (5 min each), and placed into 8% SDS in PBS (pH 8.4) at 37 °C for clearing. The detergent solution was changed daily until the tissue became evenly transparent. The cleared sections were washed in PBS (4 times, 2-3 hrs each) to fully remove SDS.

To visualize the projections of PPN ChAT neurons, we performed immunostaining with GFP antibody and TH antibody in 1 mm thick PACT-cleared brain sections. The cleared brain sections were incubated in 15 ml 0.1% Triton-X 100 / PBS, containing GFP antibody (1:250, rabbit anti-GFP, Life Technologies) and TH antibody (1:200, mouse anti-TH, Santa Cruz) at room temperature for 36 hrs, and then transferred into fresh antibody solution for 48 hrs incubation. Next, the sections were immersed in 40 ml 0.1% Triton-X 100 / PBS for 48 hrs, exchanging the solution twice daily. After washout of primary antibodies, the brain sections were incubated in 15 ml 0.1% Triton-X 100 / PBS, containing secondary antibodies (1:500, Alexa 488-conjugated donkey anti-rabbit antibody, Jackson ImmunoResearch Lab; 1:500, Alexa 647-conjugated donkey anti-mouse antibody, Jackson ImmunoResearch Lab) at room temperature for 48 hrs (fresh solution exchanged daily). The secondary antibodies were washed with the same procedure as for primary antibodies. Finally, the sections were tissue dried, immersed in 15 ml RIMS overnight or until transparent, mounted into a frame (Length-width-depth: 22x30x2 mm) (iSpacer, SunJin Lab) attached to a glass slide, immersed in RIMS (refractive index = 1.46-1.47), and coverslipped.

Confocal microscopy

Low and high magnification images were acquired with a Zeiss LSM 780 confocal microscope, equipped with: 10x Plan Apochromat air objective (NA, 0.45), 25x Plan Apochromat water immersion objective (NA, 1.2), and five laser lines (405 nm, 458 nm, 488 nm, 561 nm, and 633 nm). The microscope was controlled by Zen 2011 acquisition software (Zeiss), enabling automatic tiling and z-stacking. The images were processed with Image J (Schneider et al., 2012) and IMARIS (Bitplane).

Behavioral Assays

The rats were singly-housed in the testing room with a 12 hrs light/dark cycle (lights-on: 6 PM). Before the start of behavioral testing, subjects were handled for 3 days (10 min per day), and were granted 10 min free exploration in each behavioral apparatus. The behavioral apparatuses were sanitized with Accel between subjects.

Open field

Each 25-min open field test session consisted of a 10-min habituation to the open field box (50 x 50 cm^2), a 5-min epoch of baseline locomotor activity recording, a 5-min light-on epoch to record the effect of optogenetic modulation, and a 5-min light-off epoch to observe the recovery to baseline activity. To deliver light to photo-excite ChR2-expressing neurons or photo-inhibit Arch3-expressing neurons, we used custom-made patch cables (materials: Multimode FC/PC Connectors, 300 μm optical fiber with 0.39 NA, from ThorLab) (Sparta et al., 2012) to connect the subject's optical fiber implants to a light source (MLL-FN-473 nm /150 mW Laser or MGL-FN-532 nm/200 mW laser, from Changchun New Industries Optoelectronics Technology). The laser units were triggered by a programmable stimulator (Master 9, AMPI). For photo-excitation, we used 10 ms blue light (473 nm) pulses because 10 ms depolarization-induced spikes showed the least variability (Fig. S2C) and 10 ms photostimulation evoked spikes with precise timing (standard deviation of spike delay < 2 ms) (Fig. 3H). For photo-inhibition, we used 2 or 5 min constant green light (532 nm).

The locomotor activity was acquired with a video camera controlled by Ethovision XT 9 software (Noldus Information Technology) (Noldus et al., 2001). The data were analyzed off-line using Ethovision subject tracking capabilities to quantify the distance that the rats traveled in real-time. The software enables us to divide the square open field arena evenly into 16 (4x4) equal square fields, and to define the 4 squares in the center as the center field, and those in the periphery as the side field. To reliably track the subjects, we used the differentiating feature of Ethovision to detect the subject in the open field; the contrast, size, and contour of the detection areas were adjusted by the user to match the size of the subjects. The time that the body center of the subject enters the center and side fields was scored.

As rodents naturally prefer the periphery fields to the center field, the increase of time spent in the center field or the ratio of distance they travel in the center vs. total field can indicate anxiolysis, while decrease of these parameters usually is associated with anxiogenic effects (Cai et al., 2014; Prut and Belzung, 2003). Therefore, we used the time that the rats travel through or stay in the center field to evaluate whether optogenetic modulation affects anxiety status which may confound its modulation of locomotion or reward behaviors.

For optical stimulation, we limited the light intensity for blue (473 nm, 10 ms pulse-width at 20 Hz for 5 min) and green (532 nm, continuous light for 5 min) to levels that did not change locomotion in mCherry rats: to ≤ 6.4 and ≤ 4.5 mW / mm^2 (0.5 mm below the tip of the optical fibers) respectively. The intensity of the laser beam from the output of the patch cable (I_{cable}) was measured with an optical power meter (PM100D, ThorLab), and the intensity of light at the tip of an optical implant in brain tissue was calculated by the multiplication of I_{cable} with light transmission coefficient of each implant. Then, it was converted to light intensity (mW/mm^2) using the calculator at http://web.stanford.edu/group/dlab/cgi-bin/graph/chart.php (Aravanis et al., 2007).

Conditioned place preference / aversion

The apparatus (Fudala et al., 1985) (50×75 cm^2) has 3 compartments with white flooring throughout. The dark compartment (50×30 cm^2) has dark-gray walls with black stripes, and the white compartment (50×30 cm^2) has white walls. The white and dark compartments are

connected with staggered doorways to a middle neutral hallway (50×15 cm^2), which has a dark-gray wall facing the doorway of the dark compartment, and a white wall facing the doorway of the white compartment.

On the first day of testing (pre-conditioning session), rats were given free access to explore all 3 compartments in a 15-min session. Based on these data, a baseline place preference is calculated (time in white and dark compartment) (Fig. S5A).

On the 2^{nd} - 5^{th} days (conditioning session), a biased light-conditioning paradigm (Prus et al., 2009) was applied. To avoid ceiling and floor effects, we paired photo-excitation (blue light in ChR2 rats) to conditioning in the non-preferred (white) compartment and photo-inhibition (green light in Arch3 rats) to conditioning sessions in the preferred (dark) compartment (Fig. 4E; Fig. S5A). For the control cohort, mCherry rats were exposed to blue light pulses during conditioning in the white compartment, or to continuous green light during conditioning in the dark compartment, respectively (Fig. 4E). We used the same parameters to deliver blue (10 ms pulses at 20 Hz) and green (constant) light as those used in open field tests. To minimize overheating during light-conditioning, we alternated 5 min light-on epochs with 5-min light-off epochs during the entire 30-min conditioning session. All subjects underwent light-conditioning sessions in the morning (8:00 AM to 12:00 PM), in which their entry into the hallway and opposite chamber was blocked. Then, subjects underwent a second 30-min conditioning session to the opposite compartment in the afternoon (1:00 PM to 5:00 PM). Here, rats were connected to the patch cables, but no light was delivered to the fiber implants during this 30-min conditioning session. As before, their entry into the hallway and light-paired compartment was obstructed. For modulation of ChAT terminals in the vSNc and VTA, we applied 1 min blue light (10 ms pulses at 20 Hz, for photo-excitation) with 1 min intervals for 30 min; or 2 min green light (continuous, for photo-inhibition) with 2 min intervals for 30 min.

On the 6^{th} day (post-conditioning session), the rats were allowed to freely explore the 3 compartments. An increase in the total time that a subject spends in light-paired compartment represents the establishment of conditioned place preference, while a decrease in the total time that a subject spends in light-paired side represents the development of conditioned place aversion. The statistical significance of conditioned behaviors was assessed using the paired student's *t*-test for data of normal distribution, or else, signed rank test. To account for the possibility that light delivery alone may introduce unanticipated artifacts on place preference / aversion, ChR2/Arch3 group data for the time spent in light-paired compartment were compared to mCherry group data using the student's *t*-test or Mann-Whitney sum rank test. We did normality and equal variance analysis first in data analysis, and select *t*-test or rank test when *p* values of these analysis are greater or less than 0.05, respectively.

That rats initially showed preference to dark compartment (Fig. S5A) might suggest that their emotional status (such as, anxiety) may differ in these compartments, and changes of the place preference are associated with reduced or increased anxiety levels by photo-modulation. As the time spent in the center versus the sides of the open field arena is a demonstrated indicator of relative anxiety levels (Cai et al., 2014; Prut and Belzung, 2003), we performed this assay (see Open Field test methods), and observed that optogenetic modulation in the PPN did not change

the time the rats spent in the center area of the open field arena (Fig. S4F, L), suggesting that anxiety was not affected by photo-modulation.

Chemicals and applications

Chemicals were purchased from Sigma-Aldrich (St. Louis, MO). Mecamylamine (MEC), bicuculline (Bic), atropine, (2R)-amino-5-phosphonovaleric acid (APV), and 6-cyano-7-nitroquinoxaline-2,3-dione (CNQX) were purchased from Tocris. Stock solutions (> 1000×) were made, aliquoted and stored at 4 or -20 ºC. The final dilutions were freshly made before experiments.

Statistical analysis

Statistical analysis was performed with SigmaPlot 11.0 (SPSS Inc.) and OpenEpi Version 2.3.1 (Dean et al., 2010). We did an initial tests with a sample size of 5, calculated variation (standard deviation) of the parameters, and used the power analysis function in SigmaPlot 11.0 software to estimate the sample sizes in order to obtain reliable statistics. For statistics, values of $p < 0.05$ were considered significant. '*' and '**' in the figures respectively represent *p* values less than 0.05 and 0.01, respectively.

References

Aravanis, A.M., Wang, L.P., Zhang, F., Meltzer, L.A., Mogri, M.Z., Schneider, M.B., and Deisseroth, K. (2007). An optical neural interface: in vivo control of rodent motor cortex with integrated fiberoptic and optogenetic technology. Journal of neural engineering *4*, S143-156.

Cai, H., Haubensak, W., Anthony, T.E., and Anderson, D.J. (2014). Central amygdala PKC-delta(+) neurons mediate the influence of multiple anorexigenic signals. Nature neuroscience *17*, 1240-1248.

Dean, A.G., Sullivan, K.M., and Soe, M.M. (2010). OpenEpi: Open Source Epidemiologic Statistics for Public Health, Version 2.3.1. www.OpenEpi.com.

Fudala, P.J., Teoh, K.W., and Iwamoto, E.T. (1985). Pharmacologic characterization of nicotine-induced conditioned place preference. Pharmacol Biochem Behav *22*, 237-241.

Gradinaru, V., Thompson, K.R., Zhang, F., Mogri, M., Kay, K., Schneider, M.B., and Deisseroth, K. (2007). Targeting and readout strategies for fast optical neural control in vitro and in vivo. The Journal of neuroscience : the official journal of the Society for Neuroscience *27*, 14231-14238.

Kang, Y., and Kitai, S.T. (1990). Electrophysiological properties of pedunculopontine neurons and their postsynaptic responses following stimulation of substantia nigra reticulata. Brain research *535*, 79-95.

Matta, S.G., Balfour, D.J., Benowitz, N.L., Boyd, R.T., Buccafusco, J.J., Caggiula, A.R., Craig, C.R., Collins, A.C., Damaj, M.I., Donny, E.C*., et al.* (2007). Guidelines on nicotine dose selection for in vivo research. Psychopharmacology (Berl) *190*, 269-319.

Noldus, L.P., Spink, A.J., and Tegelenbosch, R.A. (2001). EthoVision: a versatile video tracking system for automation of behavioral experiments. Behavior research methods, instruments, & computers : a journal of the Psychonomic Society, Inc *33*, 398-414.

Paxinos, G., and Watson, C. (2006). The Rat Brain in Stereotaxic Coordinates, 6th Edition (Academic Press).

Paxinos, G., and Watson, C. (2012). Paxinos and Franklin's the Mouse Brain in Stereotaxic Coordinates, 2nd edn (Academic Press).

Prus, A.J., James, J.R., and Rosecrans, J.A. (2009). Chapter 4. Conditioned Place Preference, 2nd edn (Boca Raton (FL): CRC Press).

Prut, L., and Belzung, C. (2003). The open field as a paradigm to measure the effects of drugs on anxiety-like behaviors: a review. Eur J Pharmacol *463*, 3-33.

Quinn, B., Toga, A.W., Motamed, S., and Merlic, C.A. (1995). Fluoro nissl green: a novel fluorescent counterstain for neuroanatomy. Neuroscience letters *184*, 169-172.

Schneider, C.A., Rasband, W.S., and Eliceiri, K.W. (2012). NIH Image to ImageJ: 25 years of image analysis. Nature methods *9*, 671-675.
Sparta, D.R., Stamatakis, A.M., Phillips, J.L., Hovelso, N., van Zessen, R., and Stuber, G.D. (2012). Construction of implantable optical fibers for long-term optogenetic manipulation of neural circuits. Nature protocols *7*, 12-23.

Takakusaki, K., Shiroyama, T., and Kitai, S.T. (1997). Two types of cholinergic neurons in the rat tegmental pedunculopontine nucleus: electrophysiological and morphological characterization. Neuroscience *79*, 1089-1109.

Takakusaki, K., Shiroyama, T., Yamamoto, T., and Kitai, S.T. (1996). Cholinergic and noncholinergic tegmental pedunculopontine projection neurons in rats revealed by intracellular labeling. The Journal of comparative neurology *371*, 345-361.

Treweek, J.B., Chan, K.Y., Flytzanis, N.C., Yang, B., Deverman, B.E., Greenbaum, A., Lignell, A., Xiao, C., Cai, L., Ladinsky, M.S.*, et al.* (2015). Whole-body tissue stabilization and selective extractions via tissue-hydrogel hybrids for high-resolution intact circuit mapping and phenotyping. Nature protocols *10*, 1860-1896.

Witten, I.B., Steinberg, E.E., Lee, S.Y., Davidson, T.J., Zalocusky, K.A., Brodsky, M., Yizhar, O., Cho, S.L., Gong, S., Ramakrishnan, C.*, et al.* (2011). Recombinase-driver rat lines: tools, techniques, and optogenetic application to dopamine-mediated reinforcement. Neuron *72*, 721-733.

Xiao, C., Miwa, J.M., Henderson, B.J., Wang, Y., Deshpande, P., McKinney, S.L., and Lester, H.A. (2015). Nicotinic receptor subtype-selective circuit patterns in the subthalamic nucleus. The Journal of neuroscience : the official journal of the Society for Neuroscience *35*, 3734-3746.

Yang, B., Treweek, J.B., Kulkarni, R.P., Deverman, B.E., Chen, C.K., Lubeck, E., Shah, S., Cai, L., and Gradinaru, V. (2014). Single-Cell Phenotyping within Transparent Intact Tissue through Whole-Body Clearing. Cell *158*, 945-958.

Ye, J.H., Zhang, J., Xiao, C., and Kong, J.Q. (2006). Patch-clamp studies in the CNS illustrate a simple new method for obtaining viable neurons in rat brain slices: glycerol replacement of NaCl protects CNS neurons. J Neurosci Methods *158*, 251-259.